

Research paper

A new coordination polymer constructed from $\text{Pb}(\text{NO}_3)_2$ and a benzylideneisonicotinohydrazide derivative: Coordination-induced generation of a π -hole towards a tetrel-bonding stabilized structure



Ghodrat Mahmoudi ^{a,*}, Ardavan Masoudiasl ^a, Farhad Akbari Afkhami ^b, Jonathan M. White ^c, Ennio Zangrando ^d, Atash V. Gurbanov ^{e,f}, Antonio Frontera ^{g,*}, Damir A. Safin ^{h,i,j,*}

^a Department of Chemistry, Faculty of Science, University of Maragheh, P.O. Box 55181-83111, Maragheh, Iran

^b Department of Chemistry and Biochemistry, The University of Alabama, Box 870336, 250 Hackberry Lane, Tuscaloosa, AL, 35487, USA

^c BIO-21 Molecular Science and Biotechnology, University of Melbourne, Parkville, Victoria, 3052, Australia

^d Department of Chemical and Pharmaceutical Sciences, University of Trieste, Via L. Giorgieri 1, 34127 Trieste, Italy

^e Centro de Química Estrutural, Instituto Superior Técnico, Universidade de Lisboa, Av. Rovisco Pais, 1049-001 Lisboa, Portugal

^f Department of Chemistry, Baku State University, Z. Khalilov str. 23, AZ 1148 Baku, Azerbaijan

^g Departament de Química, Universitat de les Illes Balears, Ctra de Valldemossa km 7.5, 07122 Palma de Mallorca, Baleares, Spain

^h University of Tyumen, Volodarskogo Str. 6, 625003 Tyumen, Russian Federation

ⁱ Kurgan State University, Sovetskaya Str. 63/4, 640020, Russian Federation

^j Innovation Center for Chemical and Pharmaceutical Technologies, Ural Federal University named after the First President of Russia B.N. Eltsin, Mira Str. 19, Ekaterinburg 620002, Russian Federation

ARTICLE INFO

Article history:

Received 5 February 2021

Accepted 15 February 2021

Available online 25 February 2021

Keywords:

Lead(II)
Isonicotinohydrazide
Coordination polymer
Crystal structure
DFT

ABSTRACT

We report on a new Pb(II) coordination polymer $[\text{Pb}(\text{HL})(\text{NO}_3)_2]_n$ (**1**), obtained from a direct reaction of $\text{Pb}(\text{NO}_3)_2$ with *N'*-4-(dimethylamino)benzylideneisonicotinohydrazide (**HL**). The coordination sphere around the Pb(II) cation is built by the 1,4-*N,O*-chelating neutral **HL**, by six oxygen atoms from three chelating nitrate anions, and by the pyridyl nitrogen donor from a symmetry related molecule. The ligand **HL** and one of the nitrate anions, acting as bridging species, yield two 1D zig-zag polymeric chains along the crystallographic axes *b* and *c*, respectively. As a result, the overall structural architecture of **1** is a 2D layer, which is reinforced by the N-H...O hydrogen bonds and by $\pi \cdots \pi$ interactions, resulting in a 4-connected uninodal **sq1**/Shubnikov tetragonal plane net topology or a 3,5-connected binodal **3,5L1** net, once the N-H...O hydrogen bonds are considered. In addition of these conventional interactions, the coordination of the hydrazide group to the Pb(II) ion provokes the formation of a π -hole at the carbonyl group that establishes a tetrel bond with the oxygen atom of a nearby nitrate-ligand belonging to another polymeric chain. This interaction has been studied energetically at the PBE0-D3/def2-TZVP level of theory and also characterized by using a combination of MEP, QTAIM and NCIplot computational tools.

© 2021 Elsevier B.V. All rights reserved.

1. Introduction

During the past few decades, design and fabrication of coordination polymers (CPs) gain significant attention because of their potential usage in catalytic reactions [1,2], luminescence [3], magnetic materials [4], photovoltaic conversion [5–7] and gas sensors [8]. The large ionic radius of Pb(II) and the presence of $6s^2$ lone electron pair lead the metal to exhibit a wide range of coordina-

tion numbers being affected by the hemi- or holodirected coordination geometry and the stereoactive electron lone pairs might play a crucial role in forming various topological structures not exhibited by the d-block transition metals [9–11]. Beside coordination bonds, CPs also comprise other non-covalent bonds such as hydrogen bonds, $\pi \cdots \pi$ stacking or van der Waals interactions, resulting in their structural diversity. Few years ago researchers have coined the term «tetrel bonding» to highlight little-studied but powerful non-covalent bonding between electron donors and the group 14 elements, that energetically is comparable to hydrogen bonds and other σ -hole-based interactions [12–15]. These tetrel interactions are often crucial in the self-assembly of Pb(II) coordination polymers. Because of these characteristics, the coordination preference

* Corresponding authors.

E-mail addresses: ghodratmahmoudi@gmail.com (G. Mahmoudi), toni.frontera@uib.es (A. Frontera), damir.a.safin@gmail.com (D.A. Safin).

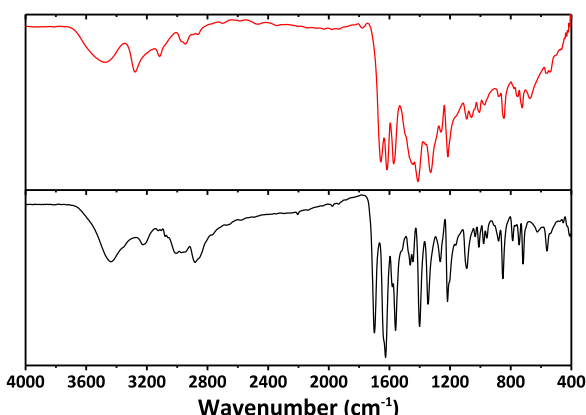


Chart 1. Diagrams of the *N'*-4-(dimethylamino)benzylidene(picolino/nicotino/isonicotino)hydrazide (**HA**), *N'*-1-(4-(dimethylamino)phenyl)ethylidene(picolino/nicotino/isonicotino)hydrazide (**HB**) and *N'*-(4-(dimethylamino)phenyl)(phenyl)methylene(picolino/nicotine/isonicotino)hydrazide (**HC**).

of Pb(II) ion and its geometry are expected to be highly sensitive to the selection of organic linkers and counter-ions [16–22]. Chelating-bridging ligands based on hydrazone-pyridine could potentially coordinate to the metal centers through their chelating fragment along with their pyridyl nitrogen atoms (bridging agent). Moreover, their amide groups could potentially interact with each other through hydrogen bonding, which is important for the construction of supramolecular arrays.

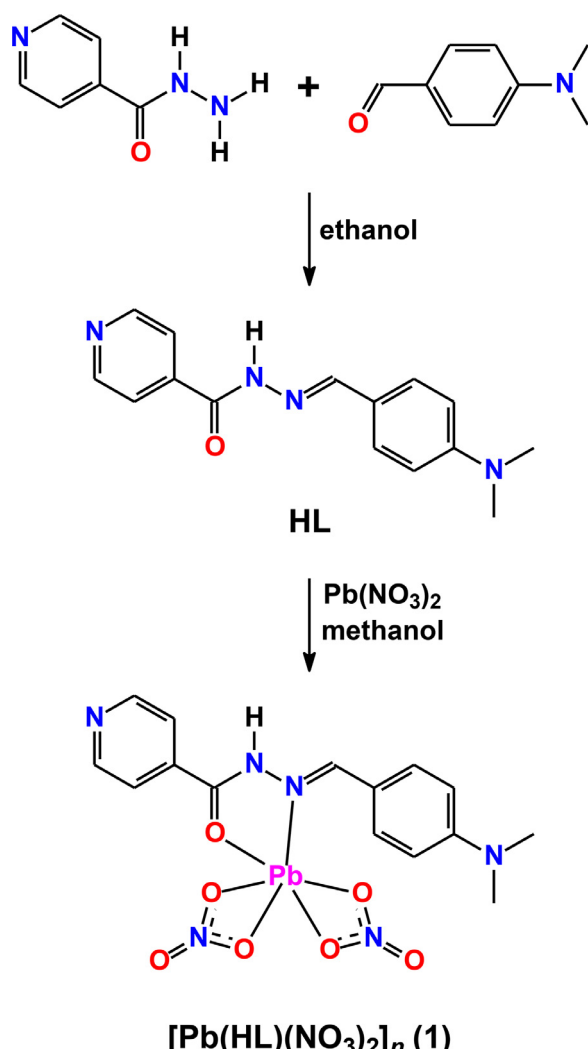
With all this in mind and in continuation of our ongoing interest in the coordination chemistry of the Pb(II) cation [23–27], as well in study the role of non-covalent interactions in the formation of extended structures, we have directed our attention to the *N'*-4-(dimethylamino)benzylideneisonicotinohydrazide (**HL**) ligand. **HL** belongs to a family of hydrazone derivatives, *N'*-4-(dimethylamino)benzylidene(picolino/nicotino/isonicotino)hydrazide (**HA**), *N'*-1-(4-(dimethylamino)phenyl)ethylidene(picolino/nicotine/isonicotino)hydrazide (**HB**) and *N'*-(4-(dimethylamino)phenyl)(phenyl)methylene(picolino/nicotine/isonicotino)hydrazide (**HC**) (Chart 1). A search in the Crystal Structure Database [28] retrieved only six crystal structures of metallocomplexes exclusively with **HA**, of which no crystal structures with Pb(II) were found. Thus, the coordination chemistry of Pb(II) with benzylidenehydrazide derivatives **HA**, **HB** and **HC** has not been explored and it is of particular interest to clarify the interactions occurring in solid state of these compounds.

In this work we have shed light on the crystal structure of a new Pb(II) coordination polymer, $[\text{Pb}(\text{HL})(\text{NO}_3)_2]_n$ (**1**), which was readily obtained by self-assembly of $\text{Pb}(\text{NO}_3)_2$ with **HL**. In addition, we describe the effect of the coordination of **HL** to Pb(II) via both the hydrazido and the pyridine moieties on the electronic nature of the hydrazido group, particularly focusing on the formation of a π -hole over the carbonyl carbon atom. The energetic features and the characterization of the C...O π -hole tetrel bonding interaction are described in the theoretical part of this work.

2. Experimental

2.1. Materials and physical measurements

All reagents were provided from commercial sources and used without further purification. Infrared spectra (KBr pellets) were recorded with a JASCO-680 spectrometer in the range 400–4000 cm^{-1} . Microanalyses were performed using a LECO-elemental analyzer.



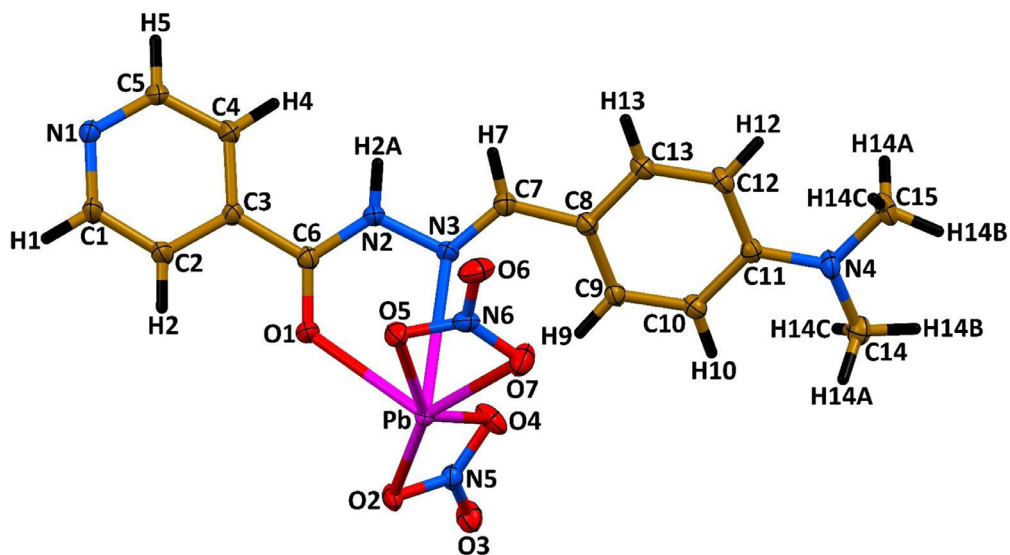
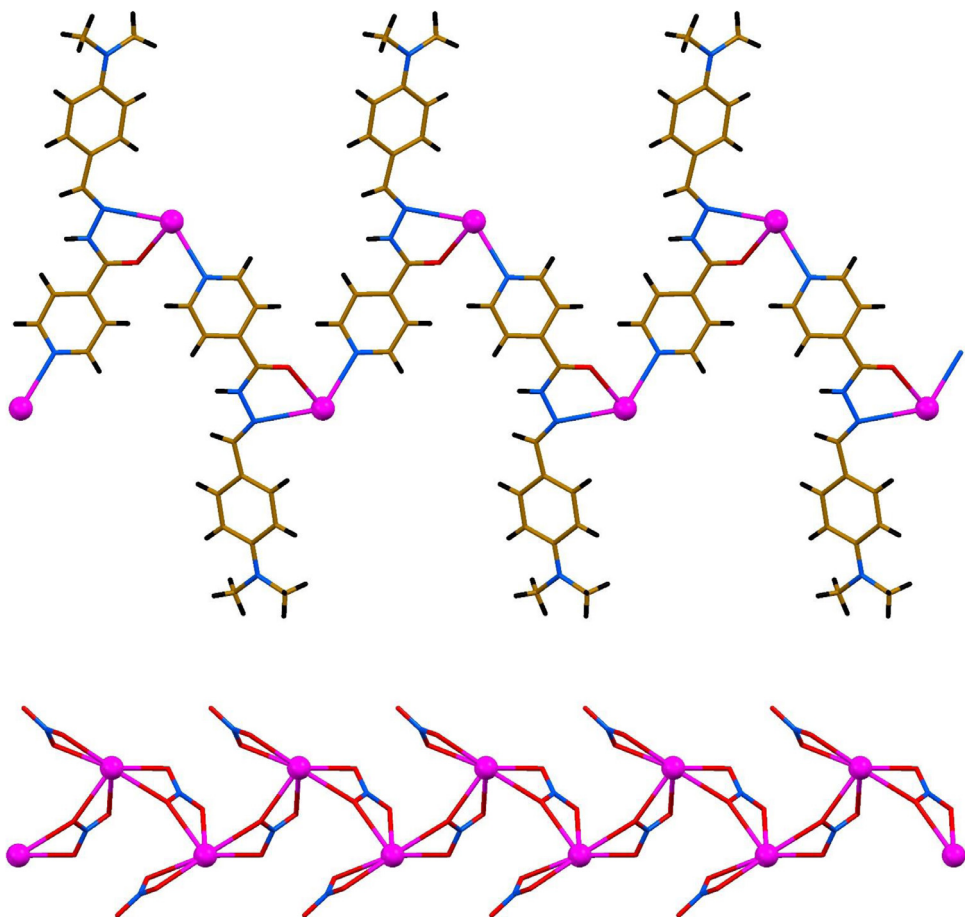
Scheme 1. Synthesis of **HL** and **1**.

2.2. Synthesis of **HL**

A mixture of 4-dimethylaminobenzaldehyde (0.149 g, 1 mmol) and isonicotinohydrazide (0.137 g, 1 mmol) in ethanol (30 mL) was refluxed for 12 h. The resulting precipitate was filtered off, washed with ethanol and dried in air. Yield: 0.228 g (85%). M.p.: 201–203 °C. Anal. Calc. for $\text{C}_{15}\text{H}_{16}\text{N}_4\text{O}$ (268.32): C 67.15, H 6.01 and N 20.88%; found: C 67.69, H 5.89 and N 20.59%.

2.3. Synthesis of **1**

The synthesis was carried out using a branched tube method [29] as previously used in these labs [21]. A mixture of $\text{Pb}(\text{NO}_3)_2$ (0.331 g, 1 mmol) and **HL** (0.268 g, 1 mmol) was placed in the main arm of the branched tube, and methanol (25 mL) was carefully added to fill the arms. The tube was sealed and immersed in an oil bath at 60 °C, while the branched arm was kept at ambient temperature. After few days, brown block-like X-ray suitable crystals were formed in the cooler arm. Crystals were isolated by filtration and dried in air. Yield: 0.354 g (59%). M.p.: 298–300 °C. Anal. Calc. for $\text{C}_{15}\text{H}_{16}\text{N}_6\text{O}_7\text{Pb}$ (599.53): C 30.05, H 2.69 and N 14.02%; found: C 29.88, H 2.76 and N 14.08%.

**Fig. 1.** FTIR spectra of **HL** (black) and **1** (red).**Fig. 2.** Crystal structure of the asymmetric unit of **1**.

2.4. Single-crystal X-ray diffraction

Diffraction data were collected at 100(1) K, using a MX2 beamline[0] Australian Synchrotron ($\lambda = 0.71073 \text{ \AA}$). Cell refinement, indexing, and scaling of the data sets were performed using the XSD program [30]. The structure was solved by direct methods [31]. Non-hydrogen atoms were refined by full-matrix least-

squares on F^2 with anisotropic displacement parameters using the program SHELXL-2014/7 [31]. Hydrogen atoms were placed at calculated positions except that at N2 located on the Fourier map and refined.

Crystal data: $C_{15}H_{16}N_6O_7Pb$, $M_r = 599.53 \text{ g mol}^{-1}$, monoclinic, space group $P2_1/c$, $a = 19.743(4)$, $b = 12.236(2)$, $c = 7.6650(15) \text{ \AA}$, $\beta = 98.56(3)^\circ$, $V = 1831.1(6) \text{ \AA}^3$, $Z = 4$, $\rho = 2.175 \text{ g cm}^{-3}$, $\mu(\text{Mo-K}\alpha) = 10.8 \text{ mm}^{-1}$, $T = 100(1) \text{ K}$.

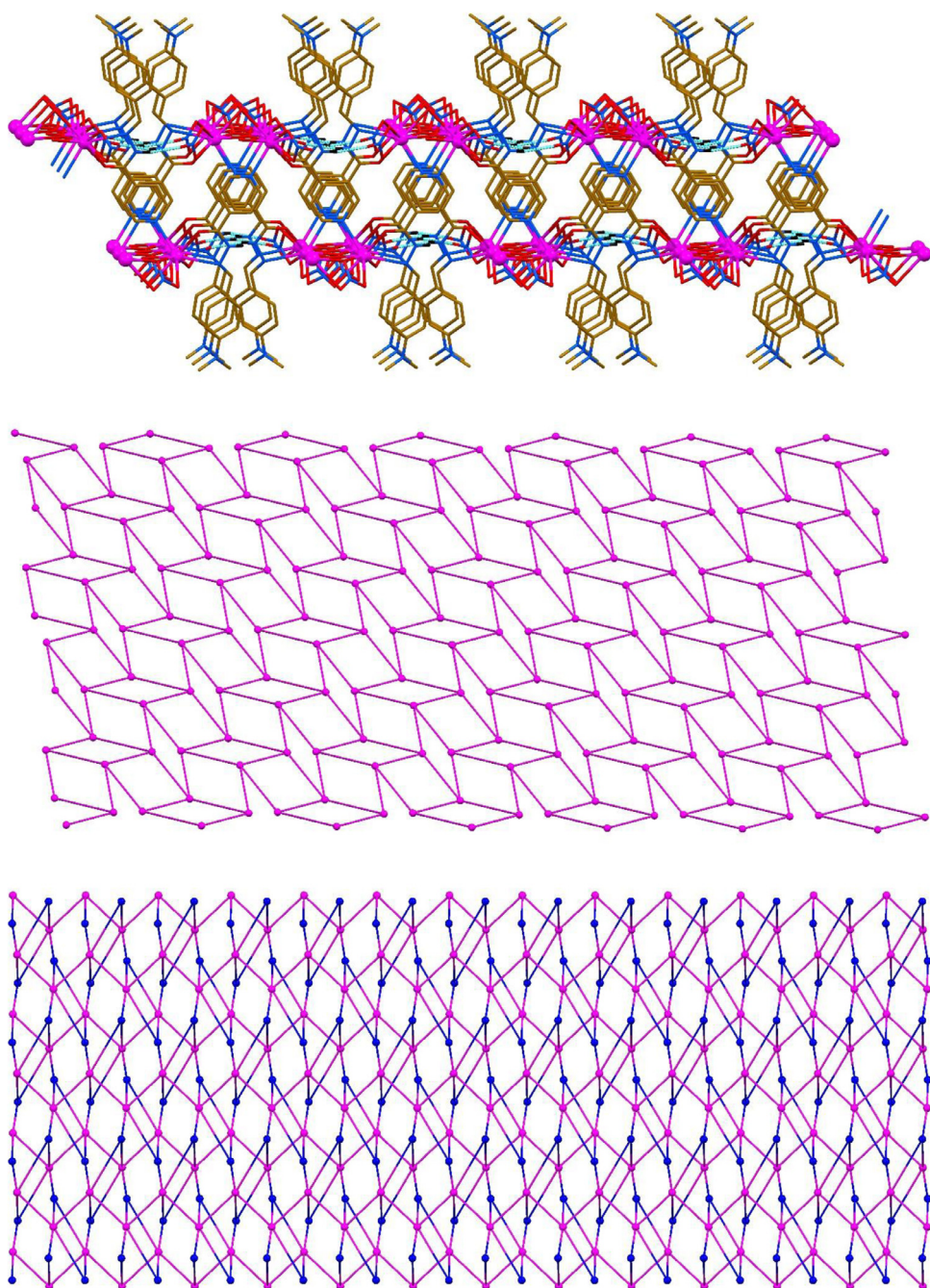


Fig. 3. (top) View of the 1D polymeric chain $[\text{Pb}(\text{HL})]_n$, developed along crystallographic axis b in the crystal structure of **1**. (bottom) View of the 1D polymeric chain $[\text{Pb}(\text{NO}_3)_2]_n$, developed along crystallographic axis c in the crystal structure of **1**. Color code: N = blue, O = red, Pb = magenta.

$\text{K}\alpha$) = 9.269 mm⁻¹, reflections: 32,711 collected, 4697 unique, $R_{\text{int}} = 0.037$, $R_1(\text{all}) = 0.0288$, $wR_2(\text{all}) = 0.0732$, $S = 1.113$.

CCDC 2041087 contains the supplementary crystallographic data. These data can be obtained free of charge via <http://www.ccdc.cam.ac.uk/conts/retrieving.html>, or from the Cambridge Crystallographic Data centre, 12 Union Road, Cambridge CB2 1EZ, UK; fax: (+44) 1223–336–033; or e-mail: deposit@ccdc.cam.ac.uk.

2.5. Theoretical methods

The non-covalent interactions were analyzed energetically using Gaussian-16 [32] at the PBE0-D3/def2-TZVP level of theory. The

binding energies have been corrected using the Boys and Bernardi counterpoise method [33]. The Grimme's D3 dispersion correction has been also used in the calculations [34]. To evaluate the interactions in the solid state, the crystallographic coordinates were used and only the position of the hydrogen bonds has been optimized. This methodology and level of theory have previously been used to analyze non-covalent interactions in the solid state [35,36]. The interaction energies were estimated by calculating the difference between the energies of the isolated monomers and the ones of their assembly. The QTAIM analysis [37] and NCiplot index [38] have been computed at the same level of theory by means of the AIMAll program [39].

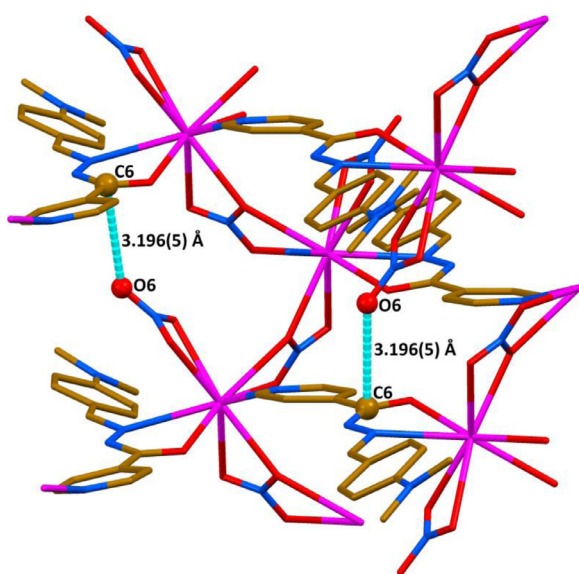


Fig. 4. (top) View of the crystal packing of **1**. Color code: H = black, C = gold, O = red, Pb = magenta; cyan dashed line = N-H...O hydrogen bond. (middle) A simplified network of **1** with the 4-connected uninodal **sql**/Shubnikov tetragonal plane net topology defined by the point symbol of $(4^4 \bullet 6^2)$. Color code: Pb = magenta. (bottom) A simplified network of **1**, considering N-H...O hydrogen bonds, with the 3,5-connected binodal **3,5L1** net topology defined by the point symbol of $(4 \bullet 5 \bullet 6)(4 \bullet 5^5 \bullet 6^3 \bullet 7)$. Color code: Pb = magenta, **HL** = blue.

3. Results and discussion

Interaction of $\text{Pb}(\text{NO}_3)_2$ and **HL** in the MeOH medium has allowed to produce a new heteroleptic CP **1** (**Scheme 1**) in the form of brown air- and moisture-stable block-like crystals. The isolated complex **1** was successfully characterized by the means of micro-analysis, FTIR spectroscopy and single-crystal X-ray diffraction. According to the FTIR spectroscopy data, the parent organic ligand presents in its neutral form in the structure of **1** as evidenced from the broad band centered at about 3460 cm^{-1} , corresponding to the NH group (**Fig. 1**). The same group in the spectrum of free **HL** was found at the same wavenumber (**Fig. 1**). Notably, the absorption band of the C=O group of the ligand **HL** in the structure of **1** is about 40 cm^{-1} shifted to low frequencies relative to that in the FTIR spectrum of free **HL**. This strongly supports its participation in the coordination towards the Pb(II) cation upon complexation. Finally, the NO_3^- anions were found in the IR spectrum of **1** as a band at about 1450 cm^{-1} (**Fig. 1**).

Complex **1** crystallizes in monoclinic space group $P2_1/c$ with one complex molecule $[\text{Pb}(\text{HL})(\text{NO}_3)_2]$ in the asymmetric unit (**Fig. 2**). The Pb(II) cation is coordinated by the 1,4-N,O-chelating **HL** and by six oxygen atoms from three nitrate anions. The coordination sphere is filled by the pyridyl nitrogen atom from a symmetry related molecule, thus, yielding a nonacoordinate environment, where the Pb(II) atom shows a holodirected coordination sphere. Notably, the nitrate anions coordinate the metal in different modes: one is simply chelating, while the other is bridging/chelating, and thus the structural features of **1** are largely determined by the crystal chemical behavior of the nitrate groups [40]. The Pb-N and Pb-O bond distances range from $2.536(3)$ to $2.864(4)$ Å with the longest one pertaining to the nitrogen atom of the isonicotinamide moiety (**Table 1**). The ligand **HL** is twisted with a dihedral angle of about 32° between the planes formed by the pyridine and phenyl rings (**Table 1**). Due to the bridging/chelating coordination mode of **HL** and one of the nitrate anions, two different 1D zig-zag polymeric chains are produced along the crystallographic axes *b* and *c* with the shortest Pb...Pb separations of 9.968

Table 1
Selected bond lengths (Å) and angles (°) for **1**.

Bond lengths ^a			
Pb-N3	2.864(4)	Pb-O3_d ^{#2}	2.796(3)
Pb-N1_b ^{#1}	2.648(3)	O1-C6	1.252(4)
Pb-O1	2.536(3)	O2-N5	1.289(4)
Pb-O2	2.637(3)	O3-N5	1.236(4)
Pb-O4	2.780(3)	O4-N5	1.243(4)
Pb-O5	2.568(3)	O5-N6	1.274(4)
Pb-O7	2.810(4)	O6-N6	1.250(4)
Pb-O2_d ^{#2}	2.700(3)	O7-N6	1.246(5)
Bond angles ^a			
O1-Pb-O2	84.80(9)	O5-Pb-N3	71.42(10)
O1-Pb-O4	94.97(10)	O5-Pb-N1_b ^{#1}	81.34(10)
O1-Pb-O5	77.11(10)	O5-Pb-O2_d ^{#2}	91.92(9)
O1-Pb-O7	118.25(10)	O5-Pb-O3_d ^{#2}	125.22(9)
O1-Pb-N3	60.60(10)	O7-Pb-N3	75.74(11)
O1-Pb-N1_b ^{#1}	74.91(10)	O7-Pb-N1_b ^{#1}	113.33(10)
O1-Pb-O2_d ^{#2}	143.13(9)	O7-Pb-O2_d ^{#2}	73.32(10)
O1-Pb-O3_d ^{#2}	157.68(10)	O7-Pb-O3_d ^{#2}	82.45(10)
O2-Pb-O4	47.37(9)	N3-Pb-N1_b ^{#1}	131.54(11)
O2-Pb-O5	157.07(9)	N3-Pb-O2_d ^{#2}	148.39(10)
O2-Pb-O7	155.01(10)	N3-Pb-O3_d ^{#2}	122.65(9)
O2-Pb-N3	111.63(10)	N1_b-Pb-O2_d ^{#2}	68.64(10)
O2-Pb-N1_b ^{#1}	80.42(9)	N1_b-Pb-O3_d ^{#2}	105.81(10)
O2-Pb-O2_d ^{#2}	94.26(9)	O2_d-Pb-O3_d ^{#2}	46.66(9)
O2-Pb-O3_d ^{#2}	73.50(9)	Pb-O1-C6	122.6(3)
O4-Pb-O5	147.31(8)	Pb-O2-N5	98.5(2)
O4-Pb-O7	116.33(10)	Pb-O2-Pb_e ^{#3}	156.10(12)
O4-Pb-N3	77.05(9)	N5-O2-Pb_e ^{#3}	98.6(2)
O4-Pb-N1_b ^{#1}	127.73(10)	N5-O3-Pb_e ^{#3}	95.4(2)
O4-Pb-O2_d ^{#2}	111.36(9)	Pb-O4-N5	92.9(2)
O4-Pb-O3_d ^{#2}	66.54(9)	Pb-O5-N6	101.3(2)
O5-Pb-O7	47.42(10)	Pb-O7-N6	90.5(2)
Dihedral angles ^b			
PbNNCO...Py	15.79	Py...C ₆ H ₄	31.64(19)
PbNNCO...C ₆ H ₄	33.98		

^a Symmetry transformations used to generate equivalent atoms: #1 $-x, 1/2 + y, 3/2 - z$; #2 $x, 3/2 - y, -1/2 + z$; #3 $x, 3/2 - y, 1/2 + z$.

^b Dihedral angles between the least-square planes, formed by the corresponding rings of the same $[\text{PbHL}]^{2+}$ species.

Table 2
Hydrogen bond lengths (Å) and angles (°) for **1**.^a

D-X...A	d(D-X)	d(X...A)	d(D...A)	$\angle(DXA)$
N2-H2A...O6 ^{#1}	0.92(6)	2.04(6)	2.937(4)	166(4)

^a Symmetry transformations used to generate equivalent atoms: #1 $x, 1/2 - y, 1/2 + z$.

Table 3
 $\pi \cdots \pi$ interaction lengths (Å) and angles (°) for **1**.^{a,b}

Cg(I)...Cg(J)	d[Cg(I)...Cg(J)]	α	β	γ	slippage
Py...Py ^{#1}	3.870(2)	10.4(2)	10.5	16.6	0.703
Py...Py ^{#2}	3.870(2)	10.4(2)	16.6	10.5	1.109

^a Cg(I)...Cg(J): distance between ring centroids; α : dihedral angle between planes Cg(I) and Cg(J); β : angle Cg(I) \rightarrow Cg(J) vector and normal to plane I; γ : angle Cg(I) \rightarrow Cg(J) vector and normal to plane J; slippage: distance between Cg(I) and perpendicular projection of Cg(J) on ring I.

^b Symmetry transformations used to generate equivalent atoms: #1 $x, 1/2 - y, -1/2 + z$; #2 $x, 1/2 - y, 1/2 + z$.

and 5.222 Å, respectively (**Fig. 3**). As a result, a 2D layer structure is achieved, where the N-H...O hydrogen bonds, formed between the amide hydrogen atom and the non-coordinated oxygen atom of the terminal nitrate anion, as well as $\pi \cdots \pi$ interactions between the pyridine rings reinforced the overall structure of **1** (**Fig. 4**, **Tables 2** and **3**). This 2D layer, studied using the ToposPro software [41], results in a 4-connected uninodal **sql**/Shubnikov tetragonal plane net topology defined by the point symbol of $(4^4 \bullet 6^2)$ or a 3,5-connected binodal **3,5L1** net topology defined by the point symbol of $(4 \bullet 5 \bullet 6)(4 \bullet 5^5 \bullet 6^3 \bullet 7)$, when the N-H...O hydrogen bonds are considered (**Fig. 4**).

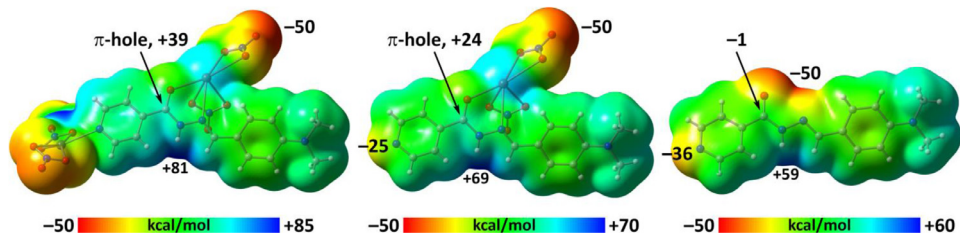


Fig. 5. Partial view of the crystal structure of **1** with indication of the C...O tetrel bonds. Hydrogen atoms were omitted for clarity. Color code: C = gold, N = blue, O = red, Pb = magenta; cyan dashed line = C...O tetrel bond.

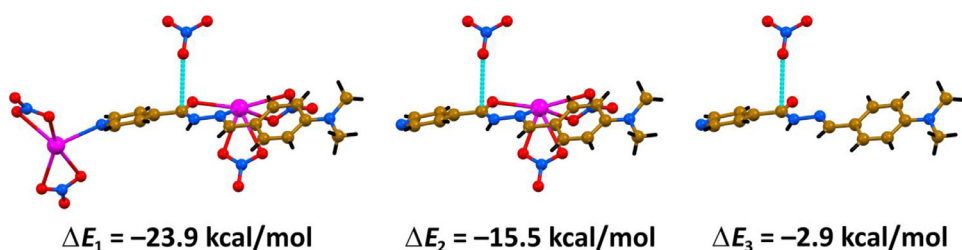


Fig. 6. MEP surfaces (isosurface 0.001 a.u.) of the theoretical models $\text{Pb}_2(\text{HL})(\text{NO}_3)_4$ (left), $\text{Pb}(\text{HL})(\text{NO}_3)_2$ (middle) and the ligand **HL** (right) at the PBE0-D3/def2-TZVP level of theory.

We have further applied the DFT (PBE0-D3/def2-TZVP) calculations to examine fine features of the crystal structure of **1**. Particularly, it was found that the C6...O6 separation of $3.196(5)$ Å is shorter than the sum of the van der Waals radii (3.22 Å), thus suggesting an attractive interaction and the apparent existence of a π -hole over the carbon atom of the hydrazido group (Fig. 5). The molecular electrostatic potential (MEP) surface of two theoretical models and the ligand **HL** have been firstly computed (Fig. 6). We have used two different monomeric models of the polymeric chain for the theoretical study. In the first model, denoted as $\text{Pb}_2(\text{HL})(\text{NO}_3)_4$, we have used two $\text{Pb}(\text{NO}_3)_2$ moieties: one monodentated (coordinated to N1) and the other one bidentate (coordinated to O1 and N3). In the second model, denoted as $\text{Pb}(\text{HL})(\text{NO}_3)_2$ only one $\text{Pb}(\text{NO}_3)_2$ moiety is bidentately coordinated to O1 and N3. In the three compounds, the maximum MEP value is located at the N-H bond, ranging from +59 to +81 kcal/mol depending on the number of Pb(II) ions coordinated to the ligand (from 0 to 2). The minimum MEP value (most negative) is located at the nitrate ligands in $\text{Pb}_2(\text{HL})(\text{NO}_3)_4$ and $\text{Pb}(\text{HL})(\text{NO}_3)_2$ models, and in the middle of the O1 and N3 atoms in the free ligand (Fig. 6). An interesting finding is that the MEP values are positive over the carbonyl carbon atom in the $\text{Pb}_2(\text{HL})(\text{NO}_3)_4$ and $\text{Pb}(\text{HL})(\text{NO}_3)_2$ models (+39 and +24 kcal/mol, respectively) and slightly negative in the ligand **HL** (Fig. 6), thus evidencing that the existence of a π -hole over the carbon atom is due to the coordination of the ligand to the Pb(II) ions.

We have also evaluated energetically the C...O interaction in the models and the free ligand. It can be observed that the interaction is very strong in the complex of $\text{Pb}_2(\text{HL})(\text{NO}_3)_4$, $\Delta E_1 = -23.9$ kcal/mol, and moderately strong in the $\text{Pb}(\text{HL})(\text{NO}_3)_2$ complex, $\Delta E_2 = -15.5$ kcal/mol (Fig. 7) in agreement with the MEP analysis. Interestingly, the interaction energy is positive (repulsive) in the NO_3^- complex with the naked ligand **HL**, $\Delta E_3 = 2.9$ kcal/mol (Fig. 7), thus strongly supporting the fact that the existence of the π -hole C...O in the solid state of **1** is caused by the coordination of the ligand to the Pb(II) metal centers. The large interaction energy obtained for the complex of nitrate with the $\text{Pb}_2(\text{HL})(\text{NO}_3)_4$ is a clear indication of the importance of this interaction in the crystal packing.

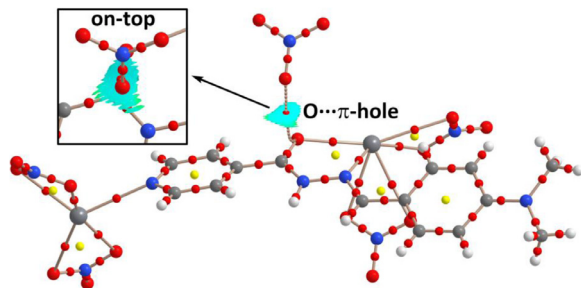


Fig. 7. Theoretical models and interaction energies of $\text{Pb}_2(\text{HL})(\text{NO}_3)_4$ (left), $\text{Pb}(\text{HL})(\text{NO}_3)_2$ (middle) and the ligand **HL** (right) interacting with the nitrate anion at the PBE0-D3/def2-TZVP level of theory. The X-ray coordinates were used for the construction of the models. Color code: H = black, C = gold, N = blue, O = red, Pb = magenta; cyan dashed line = C...O tetrel bond.

Finally, to further support the existence of the π -hole tetrel bonding interaction, we have used a combination of two methods, i.e. the quantum theory of atoms in molecules (QTAIM) and noncovalent interaction plot (NCIplot). The distribution of critical points and bond paths of the complex reveals the presence of one bond critical point and bond path (dashed line) that interconnect the oxygen atom of nitrate to the carbon atom of the carbonyl group (Fig. 8). This strange behavior of the bond path that changes the trajectory close to the carbon atom and thus interconnecting the two electron rich atoms instead the electron rich and electron poor atoms is quite common in π -hole interactions [42], because of the lack of electrons in the electrophilic atom. In this type of interaction, it is more convenient to use the NCIplot index (Fig. 8). It reveals the existence of a blue (meaning strong) surface between the oxygen and the carbon atom, in line with the energies commented above. The “on-top” representation highlighted in Fig. 8 clearly shows that the isosurface is basically located between the carbon and the oxygen atoms, thus characterizing and further evidencing the existence of the C...O tetrel bond.

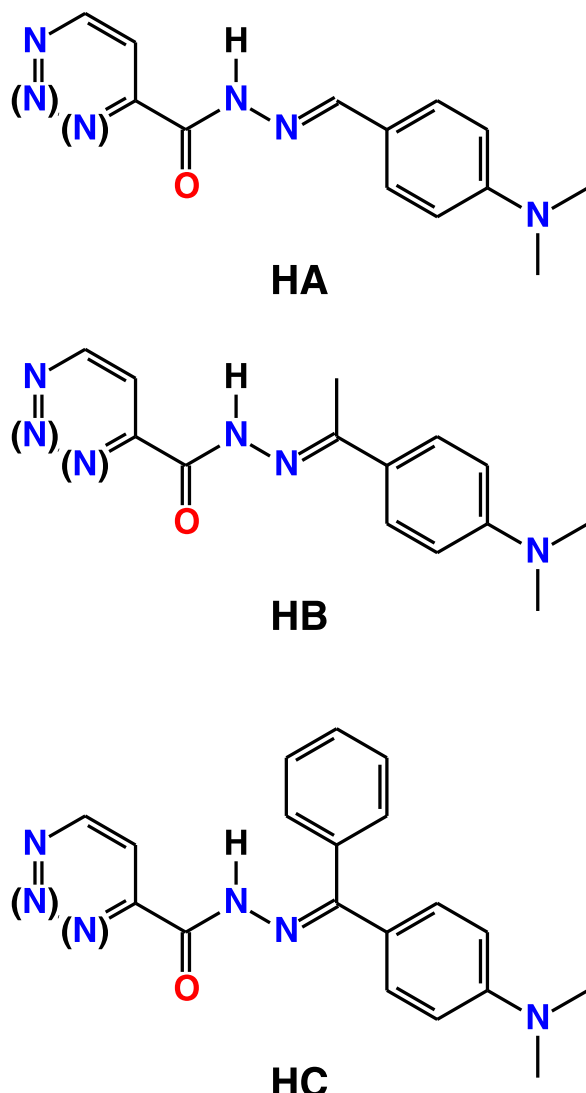


Fig. 8. Combined QTAIM (bond critical points in red and ring critical points in yellow) and NCIplot (isosurface = 0.5 a.u., $-0.02 < \text{sign}(\lambda_2)\rho < 0.04$) for the $\text{Pb}_2(\text{HL})(\text{NO}_3)_4$ model interacting with the nitrate. The NCIplot has been represented only for intermolecular interactions.

4. Conclusions

In this work we report on a new Pb(II) coordination polymer $[\text{Pb}(\text{HL})(\text{NO}_3)_2]_n$ (**1**), which was isolated from a direct reaction of $\text{Pb}(\text{NO}_3)_2$ with *N*'-4-(dimethylamino)benzylideneisonicotinohydrazide (**HL**) in the MeOH medium. According to the FTIR spectroscopy data, **HL** presents in its neutral form in the structure of **1**. Single-crystal X-ray diffraction showed that the Pb(II) is noncoordinated by the 1,4-*N,O*-chelating **HL**, six oxygen atoms of three chelating nitrate anions, and the pyridyl nitrogen atom from a symmetry related molecule. The bridging/chelating coordination mode of **HL** and one of the nitrate anions afford an overall 2D layer topology, which is reinforced by the N-H...O hydrogen bonds and $\pi \cdots \pi$ interactions, resulting in a 4-connected uninodal **sql**/Shubnikov tetragonal plane net topology or a 3,5-connected binodal **3,5L1** net, when the N-H...O hydrogen bonds are considered. In this network the two nitrate anions, acting in different coordination modes, show a critical role in the formation of this polymeric structure, leading to a holodirected coordination sphere around the Pb(II) atom.

Declarations

To be used for non-life science journals Not applicable.

Ethical Approval Not applicable.

Consent to Participate Not applicable.

Consent to Publish Not applicable.

Authors Contributions G. M. – planning research and analysis results; A. M. – conducting research and partial analysis of results; F. A. A. – conducting research; J. M. W. – planning research, analysis results, and preparing a manuscript; E. Z. – crystallography; A. V. G. – conducting research and partial analysis of results; A. F. – theoretical calculations; D. A. S. – planning research, analysis results, and preparing a manuscript.

Funding

None.

Availability of data and materials

None.

Code availability

Not applicable

Declaration of Competing Interest

The authors declare that they have no known competing financial interests or personal relationships that could have appeared to influence the work reported in this paper.

Acknowledgments

This work has been partially supported by the Fundação para a Ciéncia e a Tecnologia (FCT) 2020–2023 multiannual funding to Centro de Química Estrutural (project UIDB/00100/2020). A.V. Gurbanov acknowledges the FCT and Instituto Superior Técnico (DL 57/2016 and L 57/2017 Program, Contract no: IST-ID/110/2018). We acknowledge Australian Synchrotron for beamtime via the Collaborative Access Program (proposal 13618b). This research was funded in part by MICIU/AEI, grant number CTQ2017-85821-R, FEDER funds.

References

- [1] J.S. Seo, D. Whang, H. Lee, S.I. Jun, Y.J. Jeon, K. Kim, A homochiral metal-organic porous material for enantioselective separation and catalysis, *Nature* 404 (2000) 982–986.
- [2] Y.-B. Huang, Q. Wang, J. Liang, X. Wang, R. Cao, Soluble metal-nanoparticle-decorated porous coordination polymers for the homogenization of heterogeneous catalysis, *J. Am. Chem. Soc.* 138 (2016) 10104–10107.
- [3] S. Dey, S. Sil, B. Dutta, K. Naskar, S. Maity, P. Pratim Ray, C. Sinha, Designing of Pb(II)-based novel coordination polymers (CPs): structural elucidation and optoelectronic application, *ACS Omega* 4 (2019) 19959–19968.
- [4] D. MasPOCH, D. Ruiz-Molina, J. Veciana, Magnetic nanoporous coordination polymers, *J. Mater. Chem.* 14 (2004) 2713–2723.
- [5] A. Vogler, H. Nikol, Photochemistry and photophysics of coordination compounds of the main group metals, *Pure Appl. Chem.* 64 (1992) 1311–1317.
- [6] A. Strasser, A. Vogler, Intraligand phosphorescence of lead(II) β -diketonates under ambient conditions, *J. Photochem. Photobiol. A* 165 (2004) 115–118.
- [7] X.-Y. Zhao, B. Liang, K.-C. Xiong, Y.-W. Shi, S.-L. Yang, T.-Y. Wei, H. Zhang, Q.-F. Zhang, Y.-L. Gai, Two novel lead-based coordination polymers for luminescence sensing of anions, cations and small organic molecules, *Dalton Trans.* 49 (2020) 5695–5702.
- [8] J. López-Molino, P. Amo-Ochoa, Gas sensors based on copper-containing metal-organic frameworks, coordination polymers, and complexes, *ChemPlusChem* 85 (2020) 1564–1579.
- [9] D.-Q. Li, X. Liu, J. Zhou, Two novel extended lead(II) coordination polymers generated from bridging Schiff-base ligands, *Inorg. Chem. Commun.* 11 (2008) 367–371.

- [10] A. Aslani, A. Morsali, M. Zeller, Novel homochiral holodirected three-dimensional lead(II) coordination polymer, $[\text{Pb}_2(\mu\text{-bpa})_3(\mu\text{-NO}_3)_2(\text{NO}_3)_2]_n$: spectroscopic, thermal, fluorescence and structural studies, Solid State Sci. 10 (2008) 854–858.
- [11] M. Imran, A. Mix, B. Neumann, H.-G. Stammel, U. Monkowius, P. Gründlinger, N.W. Mitzel, Hemi- and holo-directed lead(II) complexes in a soft ligand environment, Dalton Trans. 44 (2015) 924–937.
- [12] Y.-X. Tan, F.-Y. Meng, M.-C. Wu, M.-H. Zeng, Two Pb(II) dicarboxylates constructed by rigid terephthalate or flexible d(+)-camphorate with different 3D motif based on cooperative effect of steric hindrance of ligand and lone pair electrons, J. Mol. Struct. 928 (2009) 176–181.
- [13] A. Bauzá, T.J. Mooibroek, A. Frontera, Tetrel-Bonding Interaction: rediscovered Supramolecular, Force? 52 (2013) 12317–12321.
- [14] A. Bauzá, T.J. Mooibroek, A. Frontera, Tetrel bonding interactions, Chem. Rec. 16 (2016) 473–487.
- [15] A. Bauzá, S.K. Seth, A. Frontera, Tetrel bonding interactions at work: impact on tin and lead coordination compounds, Coord. Chem. Rev. 384 (2019) 107–125.
- [16] Y.-H. Zhao, H.-B. Xu, Y.-M. Fu, K.-Z. Shao, S.-Y. Yang, Z.-M. Su, X.-R. Hao, D.-X. Zhu, E.-B. Wang, A series of lead(II)-organic frameworks based on pyridyl carboxylate acid N-oxide derivatives: syntheses, structures, and luminescent properties, Cryst. Growth Des. 8 (2008) 3566–3576.
- [17] J. Yang, J.-F. Ma, Y.-Y. Liu, J.-C. Ma, S.R. Batten, A series of lead(II) complexes with π - π stackings: structural diversities by varying the ligands, Cryst. Growth Des. 9 (2009) 1894–1911.
- [18] X.-L. Wang, Y.-Q. Chen, Q. Gao, H.-Y. Lin, G.-C. Liu, J.-X. Zhang, A.-X. Tian, Coordination behavior of 5,6-substituted 1,10-phenanthroline derivatives and structural diversities by coligands in the construction of lead(II) complexes, Cryst. Growth Des. 10 (2010) 2174–2184.
- [19] A.M.P. Peedikakkal, J.J. Vittal, Structural transformations of $\text{Pb}(\text{II})$ -trans-1,2-bis(4'-pyridyl)ethene coordination polymers in solution, Cryst. Growth Des. 11 (2011) 4697–4703.
- [20] I. Alkorta, J. Elguero, A. Frontera, Not only hydrogen bonds: other noncovalent interactions, Crystals 10 (2020) 180.
- [21] F.A. Afkhami, G. Mahmoudi, F. Qu, A. Gupta, E. Zangrando, A. Frontera, D.A. Safin, Supramolecular architecture constructed from the hemidirected lead(II) complex with N'-(4-hydroxybenzylidene)isonicotinohydrazide, Inorg. Chim. Acta 502 (2020) 119350.
- [22] G. Mahmoudi, F.A. Afkhami, A. Kennedy, F.I. Zubkov, E. Zangrando, A.M. Kirillov, E. Molins, M.P. Mitoraj, D.A. Safin, Lead(II) coordination polymers driven by pyridine-hydrazine donors: from anion-guided self-assembly to structural features, Dalton Trans. 49 (2020) 11238–11248.
- [23] G. Mahmoudi, D.A. Safin, M.P. Mitoraj, M. Amini, M. Kubicki, T. Doert, F. Locherere, M. Fleck, Anion-driven tetrel bond-induced engineering of lead(II) architectures with N'-(1-(2-pyridyl)ethylidene)nicotinohydrazide: experimental and theoretical findings, Inorg. Chem. Front. 4 (2017) 171–182.
- [24] G. Mahmoudi, A.V. Gurbanov, S.R. Hemida, R. Corballo, M. Amini, A. Bacchini, M.P. Mitoraj, F. Sagan, M. Kukulka, D.A. Safin, Ligand-driven coordination sphere-induced engineering of hybride materials constructed from PbCl_2 and bis-pyridyl organic linkers for single-component light-emitting phosphors, Inorg. Chem. 56 (2017) 9698–9709.
- [25] G. Mahmoudi, E. Zangrando, M.P. Mitoraj, A.V. Gurbanov, F.I. Zubkov, M. Moosavifar, I.A. Konyaeva, A.M. Kirillov, D.A. Safin, Extended lead(II) architectures engineered via tetrel bonding interactions, New J. Chem. 42 (2018) 4959–4971.
- [26] J.D. Velásquez, G. Mahmoudi, E. Zangrando, A.V. Gurbanov, F.I. Zubkov, Y. Zorlu, A. Masoudiasl, J. Echeverría, Experimental and theoretical study of $\text{Pb}\bullet\bullet\bullet\text{S}$ and $\text{Pb}\bullet\bullet\bullet\text{O}$ σ -hole interactions in the crystal structures of Pb(II) complexes, CrystEngComm 21 (2019) 6018–6025.
- [27] F.A. Afkhami, G. Mahmoudi, F. Qu, A. Gupta, M. Köse, E. Zangrando, F.I. Zubkov, I. Alkorta, D.A. Safin, Supramolecular lead(II) architectures engineered by tetrel bonds, CrystEngComm 22 (2020) 2389–2396.
- [28] C.R. Groom, I.J. Bruno, M.P. Lightfoot, S.C. Ward, The Cambridge Structural Database, Acta Crystallogr. B72 (2016) 171–179.
- [29] I. Wharf, T. Gramstad, R. Makhija, M. Onyszchuk, Synthesis and vibrational spectra of some lead(II) halide adducts with O-, S-, and N-donor atom ligands, Can. J. Chem. 54 (1976) 3430–3438.
- [30] W. Kabsch, XDS, Acta Crystallogr. D66 (2010) 125–132.
- [31] G.M. Sheldrick, Crystal structure refinement with SHELXL, Acta Crystallogr. C71 (2015) 3–8.
- [32] M.J. Frisch, G.W. Trucks, H.B. Schlegel, G.E. Scuseria, M.A. Robb, J.R. Cheeseman, G. Scalmani, V. Barone, G.A. Petersson, H. Nakatsuji, X. Li, M. Caricato, A. Marenich, J. Bloino, B.G. Janesko, R. Gomperts, B. Mennucci, H.P. Hratchian, J.V. Ortiz, A.F. Izmaylov, J.L. Sonnenberg, D. Williams-Young, F. Ding, F. Lipparini, F. Egidi, J. Goings, B. Peng, A. Petrone, T. Henderson, D. Ranasinghe, V.G. Zakrzewski, J. Gao, N. Rega, G. Zheng, W. Liang, M. Hada, M. Ehara, K. Toyota, R. Fukuda, J. Hasegawa, M. Ishida, T. Nakajima, Y. Honda, O. Kitao, H. Nakai, T. Vreven, K. Throssell, J.A. Montgomery Jr., J.E. Peralta, F. Ogliaro, M. Bearpark, J.J. Heyd, E. Brothers, K.N. Kudin, V.N. Staroverov, T. Keith, R. Kobayashi, J. Normand, K. Raghavachari, A. Rendell, J.C. Burant, S.S. Iyengar, J. Tomasi, M. Cossi, J.M. Millam, M. Klene, C. Adamo, R. Cammi, J.W. Ochterski, R.L. Martin, K. Morokuma, O. Farkas, J.B. Foresman, D.J. Fox, Gaussian 16 (Revision A.03), Gaussian Inc., Wallingford CT, 2016.
- [33] S.B. Boys, F. Bernardi, The calculation of small molecular interactions by the differences of separate total energies. Some procedures with reduced errors, Mol. Phys. 19 (1970) 553–556.
- [34] S. Grimme, J. Antony, S. Ehrlich, H. Krieg, A consistent and accurate ab initio parametrization of density functional dispersion correction (DFT-D) for the 94 elements H–Pu, J. Chem. Phys. 132 (2010) 154104.
- [35] P. Manna, S.K. Seth, M. Mitra, S.R. Choudhury, A. Bauzá, A. Frontera, S. Mukhopadhyay, Experimental and computational study of counterintuitive $\text{ClO}_4^- \bullet\bullet\bullet \text{ClO}_4^-$ interactions and the interplay between $\pi^+ - \pi$ and anion $\bullet\bullet\bullet \pi^+$ interactions, Cryst. Growth Des. 14 (2014) 5812–5821.
- [36] M. Mirzaei, H. Eshtiagh-Hosseini, Z. Bolouri, Z. Rahmati, A. Esmaeilzadeh, A. Bauza, P. Ballester, M. Barceló-Olivier, J.T. Mague, B. Notash, A. Frontera, Rationalization of noncovalent interactions within six new M(II)/8-aminoquinoline supramolecular complexes (M(II) = Mn, Cu, and Cd): a combined experimental and theoretical DFT study, Cryst. Growth Des. 15 (2015) 1351–1361.
- [37] R.F.W. Bader, A universal indicator of bonded interactions, J. Phys. Chem. A 102 (1998) 7314–7323.
- [38] J. Contreras-García, E. Johnson, S. Keinan, R. Chaudret, J.-P. Piquemal, D. Beratan, W. Yang, NCIPLOT: a program for plotting non-covalent interaction regions, J. Chem. Theor. Comp. 7 (2011) 625–632.
- [39] T.A. Keith, AIMAll (Version 19.02.13), TK Grismill Software, Overland Park KS, USA, 2019 aim.tkgrismill.com.
- [40] G.J. Kleywegt, W.G.R. Wiesmeijer, G.J. Van Driel, W.L. Driessens, J. Reedijk, J.H. Noordik, Unidentate versus symmetrically and unsymmetrically bidentate nitrate co-ordination in pyrazole-containing chelates. The crystal and molecular structures of [nitrate-O][tris(3,5-dimethylpyrazol-1-ylmethyl)amine]copper(II) nitrate, [nitrate-O, 2;2][tris(3,5-dimethylpyrazol-1-ylmethyl)amine]nickel(II) nitrate, and [nitrate-O][nitrate-O,O'][tris(3,5-dimethylpyrazol-1-ylmethyl)amine]cadmium (II), J. Chem. Soc., Dalton Trans. (1985) 2177–2184.
- [41] V.A. Blatov, A.P. Shevchenko, D.M. Proserpio, Applied topological analysis of crystal structures with the program package ToposPro, Cryst. Growth Des. 14 (2014) 3576–3586.
- [42] E. Escudero-Adán, A. Bauzá, C. Lecomte, A. Frontera, P. Ballester, Boron triel bonding: a weak electrostatic interaction lacking electron-density descriptors, Phys. Chem. Chem. Phys. 20 (2018) 24192–24200.